Materials Research Letters

A Methodology for Quantitatively Characterizing the Dispersion of Nanostructures in Polymers and Composites

S. Pfeifer[a] & P.R. Bandaru[a]

[a] Department of Mechanical and Aerospace Engineering, Materials Science Program, University of California, Room 258, Engineering 2, San Diego, La Jolla, CA 92093-0411, USA
Published online: 13 Feb 2014.

CrossMark

Click for updates

PLEASE SCROLL DOWN FOR ARTICLE

A Methodology for Quantitatively Characterizing the Dispersion of Nanostructures in Polymers and Composites

S. Pfeifer and P.R. Bandaru[*]

Department of Mechanical and Aerospace Engineering, Materials Science Program, University of California, Room 258, Engineering 2, San Diego, La Jolla, CA 92093-0411, USA

We seek to provide a metric for quantifying the degree of dispersion of nanostructures, such as carbon nanotubes in polymeric and other matrices, motivated by the technological importance of nanostructure-based composites. Our proposed measure of dispersion uses a quadrat-based sampling algorithm and a metric $d(P||Q)$, to correlate randomness to the dispersion. This allows a quantitative comparison of the given distribution (say, P) to a preferred distribution or pattern (say, Q). We provide examples from our own studies and those from the literature on the application of the metric.

1. Introduction It is often necessary to quantitatively measure the degree of dispersion of microscopic and nanoscopic entities in a macroscopic polymer matrix. As an example for illustrating the applicability of such a notion, composites constituted of carbon nanotubes (CNTs) placed in a polymer [1,2] have been widely proposed for electromagnetic interference shielding,[3–5] in high sensitivity infrared sensors,[6] structural applications,[7,8] etc. It has been widely accepted that the composite properties would be optimal when the CNTs are uniformly dispersed within the polymer matrix.[9] More generally, agglomeration of nanostructures/CNTs—in the bulk, surfaces/films, or on fibers/fiber surfaces—is undesirable as it promotes non-uniformity in the measured properties, whereby the characteristics would be a function of which part of the sample was measured. The uniform dispersal and bonding of CNTs in a polymer may confer unique properties to the composite, e.g. through the postulated formation of an interphase region,[10] enhanced charge carrier scattering,[11] etc. Similar considerations also apply to the dispersion of other structures such as nanoparticles,[12] e.g. used in polymer composite foams [13] where aggregation and bundling can lead to poor interfacial bonding of the structures with the polymer matrix. Bundling is not unexpected due to the strong van der Waals bonding prevalent in such structures. This in turn can cause variable and diminished properties in the composite. While single-walled CNT (SWCNT) and multi-walled CNT (MWCNT)-based composites have been reported [14–16] to have enhanced elastic modulus and ultimate tensile strength, it has been frequently seen that beyond a certain loading, fillers can be deleterious (e.g. at ∼0.6 vol% in phenol/SWCNT composites [17] or polypropylene/SWCNT composites [16]), presumably due to bundling of the CNTs. In our own studies, we have seen a decrease in the work of fracture of a SWCNT-RET (reactive ethylene terpolymer) composite at ∼0.1 vol% loading fraction of the nanotubes.[8]

It was also proposed that the nanostructure surfaces and interfaces could be functionalized through the use of suitable coupling agents [18,19] and made to interact more homogeneously with the polymer matrix. However, it is practically difficult to uniformly disperse nanostructures as the very same characteristics that confer their unique properties (e.g. high specific surface area) also encourage mutual attraction. It has also been shown [20] that commonly used homogenization techniques such as ultra-sonication/blending could destructively reduce CNT length to diameter aspect ratio. While maintaining uniformity in dispersion is difficult and is presently an active research topic, it would nevertheless be pertinent

---

[*]Corresponding author. Email: pbandaru@ucsd.edu

to understand *quantitatively* or define more definitively the degree of dispersion of nanostructures, such as CNTs, within a polymer. This paper sets out to provide such a metric suitable for quantifying the dispersion. The merit arises from the strong theoretical foundations used, where well-established information theory principles, invoking the entropy, can be adapted to understand and correlate randomness in the dispersion thereby allowing a comparison of the given distribution to a preferred distribution or pattern. We also suggest that our technique can be used for describing the dispersal of any minority phase within a majority phase.

At the very outset, the visual examination of a micrograph is inadequate to gauge the uniformity of a particular dispersion of the nano-/micro-structures within a matrix, e.g. the presence/absence of agglomerates can both indicate similar dispersion uniformity. A variety of qualitative, semi-quantitative and quantitative methodologies have then been used for the quantification of the dispersion. We first discuss ASTM (American Society for Testing and Materials) standard (D2663),[21] along with the three test methods invoked for the dispersion of carbon black type fillers in polymeric matrices. One version (Test Method A) incorporates visual inspection or linear intercept methods,[22] where the dispersion level is compared with a series of five photographic standards/comparison charts [23] and then rated numerically from 1 (poor dispersion) to 5 (very good dispersion). Alternately, in a more quantitative methodology (Test method B), the total cross-sectional area of the additive agglomerates with a spatial extent of greater than 5 μm is counted and subtracted from the known added content of the additive. The percentage of additives below the 5 μm limit is given as a measure of the dispersion, as follows: >97%—'high' dispersion, 92–97%—'intermediate' dispersion and <92%—'low' dispersion. In another semi-quantitative method (Test Method C), the cut surface of a certain sample is traced with a stylus and the amount of roughness caused by the agglomerates is translated to measure the dispersion.

Alternately, fundamental statistical measures could also be used for a dispersion index. For example, the average number (/mean) number of particles and the deviation from the mean (i.e. through the variance as in the χ^2 distribution-based tests) in a given unit could be considered. However, such measures may not be valid for low filler content and often assume an underlying Gaussian distribution. While a better measure could be obtained through considering a higher order moment about the mean, i.e. through measuring the skewness, which may be in the range of zero (for well-dispersed and uniformly distributed particles) to infinity (for large aggregates) there is an implicit reference to an expected mean number of particles per unit/quadrat which is a priori unknown. An alternate measure (valid for 0–20% CNT loading in polymer matrices) considering both the

spread of the additive (considering a *dIndex*, varying between 0 and 0.5) as well as the *size* of the additive agglomerate (through a *sIndex*, varying between 0 and 0.5) based on a quadrat [23] methodology was recently proposed.[24] The overall dispersion index was considered to be the arithmetic average of the two indices and varied between zero (maximally ill dispersed) and one (maximally well dispersed). However, the assignment of a range between zero and one, as well as considering a 'maximum particle agglomerate size' is still arbitrary and not well founded. Moreover, the notions of a range and minimal or maximal dispersion are not well defined and clearly quantifiable.

In much of the literature, the measurement of dispersion in a particular micrograph area is quantified by dividing the net area into cells (/quadrats) of equal area. While there is a basic degree of uncertainty in choosing the optimal size of the quadrat (as this choice determines the dispersion index number), it still seems to be the most meaningful basis. Alternate measures, e.g. the free-space length, L_f,[25] which correlates to the 'characteristic size of the unreinforced polymer domains' and defined as the 'width of the largest randomly placed square for which the most probable number of intersecting particles is zero' are still equivalent to measuring the mean length of the largest quadrat square likely to contain zero particles, and have a potential drawback in that a large L_f could be indicated for low volume fraction nanostructure fillers. The Morisita index,[26] which was also proposed as an alternate measure relatively independent of the quadrat size, compares images with similar objects and was shown to be inadequate for nanocomposites with similar degrees of filler mixing.[22]

The methods discussed above are based on assumptions of underlying statistical distributions (typically assumed to be normal/Gaussian), and inherently lack an objective theoretical foundation, e.g. the relevant equations are not of the logarithmic form. Such a requirement is mandated from information theory,[27] which is proposed in this paper as an attribute to be used to relate the degree of uniformity in dispersion to the probability of locating CNTs.[28] The specific advantages of our approach are evident in that we were able to (a) successfully categorize images and image distributions that could not be characterized by other indices, such as the Morisita methodology,[22] (b) produce a single metric, for quantifying the dispersion, and (c) could compare a given image to another image or a given/preferred distribution. The drawbacks may be related, as discussed earlier, to the issue of obtaining an optimal quadrat size, choosing between accuracy and computational time. An optimal quadrat square should indeed be chosen to adequately characterize the nanostructure distribution, i.e. larger quadrats can make a clustered distribution look uniform since such quadrats tend to have nearly the same number of nanostructures/CNTs, while smaller quadrats

may not contain any CNTs—also see discussion in Section 3.

2. Principles of the Approach

A suitable dispersion metric should enable a comparison with either an idealized dispersion pattern or alternatively with a desired probability distribution (e.g. uniform, Poisson distribution, etc.). From a more quantitative perspective, one example of a well-defined metric involves the use of the *quadrat* approach [22,23] which can be applied at any nanostructure fraction. In such a method, for example, the CNTs are located from a visual micrograph obtained, e.g. through transmission/scanning electron microscopy (TEM/SEM)-based images of a composite cross-section. The image is then subdivided into several squares/*quadrats* and the number of pixels corresponding to the CNTs within each quadrat counted. A perfectly uniform arrangement of the dispersants within the matrix would then exhibit an equal number of centers in each quadrat, so that deviations may be gauged, e.g. by calculating the relative entropy or the distance between the distributions.

A measure of the average randomness (/entropy) of a given composite constituted from the nanostructure (filler)—polymer (matrix) distribution is given by the average of the possible arrangements of filler (f) and matrix (m) entities (with $f + m = 100\%$ or unity) and is proportional to the total number of their arrangements, i.e. $f!m!/(f + m)!$, which can be simplified through the Stirling formula to $f \ln(f) + m \ln(m)$, where ln is the natural logarithm. The entropy of the filler-matrix ensemble for a given distribution, say P, could then be defined through [27]

$$H(P) = f_P \ln(f_P) + m_P \ln(m_P). \qquad (1)$$

Comparing such a distribution 'P' to another given nanostructure-polymer dispersion, say 'Q', whose entropy is given by $H(Q) = f_Q \ln(f_Q) + m_Q \ln(m_Q)$, we can derive a comparison function to denote the relative entropy between these two distributions, $D(P||Q)$, through [27,29]

$$D(P||Q) = H(P) - H(Q). \qquad (2)$$

This interpretation of the *relative entropy* is then illustrated with respect to how a particular nanostructure distribution, say corresponding to 'P', differs from a preferred/standard distribution corresponding to 'Q', e.g. a Poisson or uniform (square, hexagonal lattice, etc.) distribution.[24,25] In other words, $D(P||Q)$ measures the 'inefficiency of assuming that the distribution is Q, when the true distribution is P'.[27,29] A corollary of the previous statement is that when a particular distribution 'P' approaches the preferred distribution 'Q', the relative entropy should approach zero (which is the

logarithm of 1). However, $D(P||Q)$ is not a complete metric since the equality $D(P||Q) = D(Q||P)$ usually does not hold.[23] We postulate an average, i.e. $d(P||Q)$ as follows [26]:

$$d(P||Q) \equiv \frac{1}{2}[D(P||Q) + D(Q||P)] \geq 0. \qquad (3)$$

It is apparent that $d(P||Q) = d(Q||P)$ and when the distributions are equivalent, i.e. $d(Q||Q) = 0$.

3. Implementation of the $d(P||Q)$ Metric to Gauge the Uniformity of a Given CNT Distribution Within a Polymer Matrix

We will next outline the methodology for utilizing the above principles in quantifying the deviation of a given CNT distribution in a polymer from a standard distribution. Initially, an algorithm (implemented in MATLAB™) was used to generate 10,000 randomly positioned quadrats, imposed on a micrograph. Although the algorithm could have simply placed a quadrat centered at each pixel within the image, the use of such a random sample of quadrats saves computational time when evaluating larger micrographs, while providing a satisfactory representation of each image. Also, this allows the direct comparison between differently sized micrographs since the conventional approach of using a fixed quadrat grid would require a different number of quadrats for differently sized micrographs. Additionally, a fixed quadrat grid can result in significantly different dispersion metrics depending on where the grid is superimposed over the micrograph.[23,30] We note that a sufficiently large quadrat square should be chosen to adequately characterize the actual CNT distribution, e.g. if no CNT lies within a quadrat, the quadrat size should be increased until the expanded quadrat contains at least one pixel from a CNT. This is essential for Equations (2) and (3) to be well defined.

It is reiterated that the choice of quadrat size is very important in gauging the dispersion and producing a reliable d-metric. An optimal quadrat square should indeed be chosen to adequately characterize the nanostructure distribution, i.e. larger quadrats can make a clustered distribution look uniform since such quadrats tend to have nearly the same number of nanostructures/CNTs, while smaller quadrats may not contain any CNTs.

Consequently, while there is no straightforward way to determine the optimal quadrat size and shape, several empirical rules have been previously suggested, e.g. that approximately twice the mean area of a particle is suitable as the square quadrat size [31] should be used. For our study, an initial quadrat area of 45 pixels × 45 pixels, corresponding to ∼3.5 times the average particle diameter, related to the midpoint of a range of initial quadrat sizes, that gave acceptable and reproducible dispersion measurement trends, was chosen. We could modify this initial quadrat size slightly without changing the relative

ranking of dispersions in our study. The general procedure, which could be employed for gauging the *d*-metric, was as follows:

(A) Given a particular image, the numerical value of the degree of darkness of a pixel (which is the smallest element of an image) is identified with 8-bit resolution—range from 0 (black) to 255 (white). While our algorithm can also be adapted for colorized images, by assigning bin numbers to different colors, we focus on gray scale images to reduce the complexity.

(B) The pixel darkness values are obtained for the nanostructure (e.g. CNT) and the polymer through the SEM/TEM micrographs using the ImageJ® application.

(C) The pixel value threshold for distinguishing the nanostructure from the contrasting polymer background is determined from an examination of the micrographs. In most cases, a 150-pixel darkness value could distinguish CNTs from the polymer background. *It is to be expected that other images corresponding to those produced by different equipment/imaging conditions may require a different threshold.*

(D) The initial length of each quadrat square (in terms of the number of pixels) should then be set to correspond to *at least* (twice) the minimum nanostructure size, for a given magnification. As previously discussed, a small quadrat size (corresponding to a large number of quadrats on the micrograph as well as many empty quadrats) result in excessive computation time while a large quadrat size may yield inaccurate results, e.g. they may make a clustered distribution look uniform.

(E) On another note, the quadrat size should be sufficiently large to capture the nanostructures/CNTs that vary in diameter either within an image or when the magnification changes without being so large as to mask clusters of inclusions. For instance, a 30×30 pixel quadrat has a greater than 99.9% chance of containing at least one CNT pixel with perfectly distributed CNTs in a 1 vol% CNT-polymer constituted composite. Consequently, such an initial quadrat size should work well with imperfectly distributed CNTs across a range of loadings. Periodic boundary conditions should be applied to avoid preferential sampling near the image boundaries.

As in the proper reporting of any scientific measure, the dispersion uniformity must be gauged over a number of micrographs (of samples prepared under nominally identical conditions) under consistent conditions (e.g. at a given value of magnification, reported threshold

value, etc.). The utilized MATLAB® m-files comparing an (i) image to a distribution and (ii) two mutual images have been appended to the *Supplementary Information*.

Our program was then configured to yield the area fraction of the CNTs within each of the 10,000 quadrats. The CNT distribution probabilities, p_i—related to probability of finding CNTs within the *i*th quadrat, were found through using the area a_i (in units of pixels) of the CNTs within the *i*th quadrat of area A_i, through

$$p_i = \frac{a_i/A_i}{\sum_{i=1}^{n} a_i/A_i}. \qquad (4)$$

The denominator normalizes the probability over the total number (*n*) of quadrats, so that $\sum_{i=1}^{n} p_i = 1$. It is to be noted that the p_i are related to the filler (i.e. $p_i = f_{i,P}$) or the matrix (i.e. $p_i = m_{i,P}$) in a given distribution, *P*. Equation (4) can also be used as an estimator of a probability function for deterministic patterns, e.g. (i) $p_i = 1/n$, for a uniform distribution. However, of the five types of two-dimensional Bravais lattices, the hexagonal lattice could be considered the most well-dispersed since it has the largest number of equidistant nearest neighbors.[32] Consequently, for the purpose of a preferred/standard distribution a hexagonal lattice (HEX) was chosen. It is to be emphasized that our proposed approach and algorithm can be applied to any distribution, and we chose the HEX distribution only for illustrative purpose. The Uniform and the HEX distributions are similar but not identical ways to characterize dispersion. The Uniform distribution, for example, expects the same number of particle pixels circumscribed within each quadrat and that it would always be unnecessary to expand a quadrat to encompass at least one pixel. On the other hand, quadrats superimposed in a random fashion over HEX will not always contain the same number of particle pixels and a quadrat placed over an empty zone in HEX will require enlargement to encapsulate at least one particle pixel. Generally, a user is free to select an *ideal* distribution according to their needs and/or applications. For example, one user may have the flexibility to call Figure 2(a) 'ideal' for their application. Another user may prefer a HEX pattern. A third may want a UNIFORM distribution or perhaps a more stratified pattern (say, for a waveguide). Our algorithm lets the user specify their version of 'ideal' for their particular application. Although there can be different versions of what constitutes ideal, we view this flexibility as a desirable attribute of the algorithm.

It may also be desirable to change the density of the chosen/preferred pattern to represent a higher or lower volume fraction of the nanostructure dispersion. We selected an area fraction and particle diameter in HEX to illustrate a reasonable example of an 'ideal' image suitable for comparison in a study. However, the user is free to account for particle loading, magnification and particle diameter in the selection of the ideal image or distribution, e.g. by using larger or smaller diameter particles (and/or

with more or less area fraction) to represent the volume (area) fraction of inclusions of a particular diameter in a nanocomposite. Our algorithm, also allows the user to specify an equal number of particles in each quadrat as an ideal—instead of using an idealized pattern. This may be desired since deterministic patterns such as HEX may exhibit a *picture perfect* level of dispersion that may not needed for some applications. In such ways, images of nanostructures dispersed in polymers can be compared with a preferred point pattern/lattice, using Equation (4) as an estimator of the probability function. The a_i/A_i may also be considered a reasonable estimator of the CNT volume fraction.

For calculating the a_i, we had to consider carefully from digital images/micrographs the pixels that do represent CNTs. Generally, digital images are created by a quantization and sampling process, which mathematically represents an image through a matrix of real numbers. Each matrix element corresponds to a pixel which is the smallest element of the image and is identified by its position within the image and a numerical value representing the degree of darkness of that pixel.[33] In our processed images, the numerical value (with 8-bit resolution) could range from 0 (black) to 255 (white). We measured CNT and polymer

pixel values within our micrographs using the ImageJ application (http://rsbweb.nih.gov/ij/) and determined, for our case (Figure 1) that a 150 pixel value threshold could distinguish CNTs from the contrasting polymer background. Both MATLAB™ and ImageJ recognize pixels by their numerical value, and it is to be expected that other images corresponding to those produced by different equipment/imaging conditions may require a different threshold. The initial length of each quadrat square was then set to be 45 pixels which is approximately 3.5 times the average CNT diameter at $1250\times$ magnification (the exact conversion between pixels and CNT diameter would vary with the magnification [22,34]). Ten measurements of $d(P||Q)$, with respect to the HEX pattern, were averaged for any particular image/pattern under test to estimate the population average and lower the standard error estimate (as indicated in Table 1).

We then applied the above methodology to test the proposed dispersion metric, to both our own pattern images of CNTs dispersed in an epoxy polymer (RET) as well as those published in the literature.[22,25] The RET (Elvaloy 4170) was constituted of (1) polyethylene, (2) a polar methyl-methacrylate group and (3) epoxide functional groups. While (1) and (2) contribute to mechanical elastomeric characteristics and corrosion
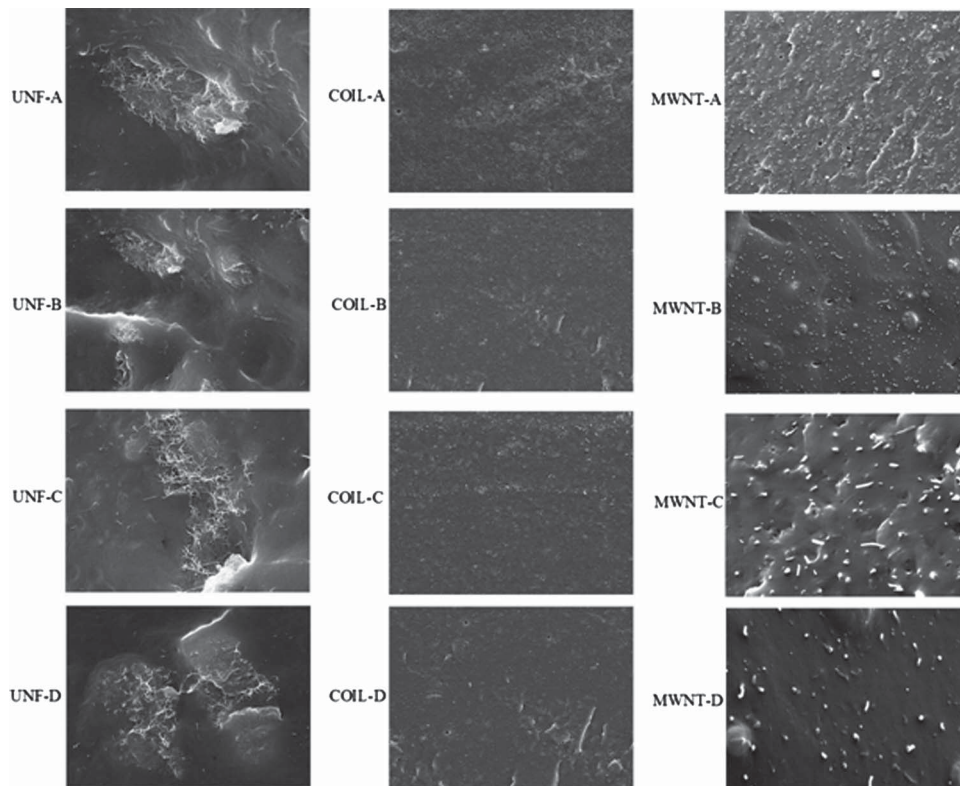
Figure 1. The uniformity of dispersion of carbon nanotubes (CNTs) dispersed in a RET polymer matrix, decreases from the top to the bottom in these SEM micrographs and a quantitative measure can be obtained through a *d*-metric analysis—Table 1. *Left column*: Increasingly poor dispersion of unfunctionalized CNTs (increasing from the top, UNF-A to the bottom, i.e. UNF-D). *Center column*: Increasingly poor dispersion of coiled CNTs (increasing from the top, COIL-A to the bottom, i.e. COIL-D). *Right column*: Increasingly poor dispersion of MWCNTs (increasing from the top, MWNT-A to the bottom, i.e. MWNT-D).

Table 1. The *d*-metric for the images in Figure 1 indicates a quantification of the degree/uniformity of dispersion.

$\langle d(\text{HEX}||\text{Pattern})\rangle$	$\langle d(\text{HEX}||\text{Pattern})\rangle$	$\langle d(\text{HEX}||\text{Pattern})\rangle$
$\langle d(\text{HEX}||\text{UNF-A})\rangle = \mathbf{5.805}(0.007)$	$\langle d(\text{HEX}||\text{COIL-A})\rangle = \mathbf{0.858}(0.004)$	$\langle d(\text{HEX}||\text{MWNT-A})\rangle = \mathbf{0.275}(0.001)$
$\langle d(\text{HEX}||\text{UNF-B})\rangle = \mathbf{5.815}(0.009)$	$\langle d(\text{HEX}||\text{COIL-B})\rangle = \mathbf{1.259}(0.011)$	$\langle d(\text{HEX}||\text{MWNT-B})\rangle = \mathbf{0.623}(0.004)$
$\langle d(\text{HEX}||\text{UNF-C})\rangle = \mathbf{6.092}(0.011)$	$\langle d(\text{HEX}||\text{COIL-C})\rangle = \mathbf{1.721}(0.015)$	$\langle d(\text{HEX}||\text{MWNT-C})\rangle = \mathbf{3.084}(0.012)$
$\langle d(\text{HEX}||\text{UNF-D})\rangle = \mathbf{6.577}(0.009)$	$\langle d(\text{HEX}||\text{COIL-D})\rangle = \mathbf{2.831}(0.007)$	$\langle d(\text{HEX}||\text{MWNT-D})\rangle = \mathbf{4.690}(0.007)$

Note: The numbers in bold indicate the *d*-metric values, the standard deviation from 10 measurements is indicated in the parenthesis.

resistance and are critical to the utility of RET as a hot-melt adhesive and coating, the epoxide group has high reactivity [19] and is amenable for effective anchoring of the constituent ring bonds with functional groups (e.g. $-\text{OH}$, $-\text{COOH}$, $-\text{NH}_2$, etc.) on the CNTs.[35] As the functional groups are associated with defects on the CNTs and are randomly dispersed, isotropic bonding of the nanotubes with the polymer matrix was implied and expected to yield relatively uniform CNT dispersion. Both pristine and $-\text{COOH}$ functionalized SWCNTs (average diameter of 1.5 nm, length range $\sim$5–20 μm), MWCNTs (average diameter of 140 nm, length range $\sim$5-9 μm), as well as coiled CNTs [36,37] were used. Further details of the dispersal procedure and structural, electrical, and electromagnetic characterization have been reported previously.[3]

Generally, considerable clumping reflective of CNT agglomeration was observed when unfunctionalized CNTs (to the left of Figure 1) were mixed into the polymer. We then observed that the general strategy of employing mutual chemical reaction between functional groups on the CNT and the polymer through covalent functionalization of the nanotube surface [38] resulted in a relatively more uniform dispersion of SWCNTs in the polymer over a wide range of nanotube volume fractions, i.e. from 0.2 to 4.5 vol% (for functionalized coiled nanotubes and multi-walled nanotubes, in the center and to the right of Figure 1, respectively). It was noted that TEM images have poor contrast between SWCNTs and the surrounding matrix and the SEM images have adequate subject contrast between the inclusions and the surroundings to demonstrate the efficacy of our dispersion algorithm.

We now characterize the extent of uniformity in the CNT dispersed RET polymer through the $d(P||Q)$ metric, as applied to SEM images of the distribution of unfunctionalized and functionalized CNTs in the polymer (Figure 1). The images in Figure 1 represent the SEM micrographs of fracture surfaces of the samples. Contrast was used to distinguish the CNTs (which are predominantly metallic) from the background roughness. More specifically, we measured CNT and polymer pixel values within our micrographs using the ImageJ® application and distinguish CNTs from the contrasting polymer background, through appropriate digital filtering. The use of

Table 2. The *d*-metric for the images in Figure 2 indicates a quantification of the degree/uniformity of dispersion.

$\langle d(\text{Uniform}||\text{Pattern})\rangle$
$\langle d(\text{Uniform}||\text{a})\rangle = \mathbf{0.021}(0.001)$
$\langle d(\text{Uniform}||\text{b})\rangle = \mathbf{0.066}(0.001)$
$\langle d(\text{Uniform}||\text{c})\rangle = \mathbf{0.153}(0.003)$
$\langle d(\text{Uniform}||\text{d})\rangle = \mathbf{1.354}(0.007)$

Note: The numbers in bold indicate the *d*-metric values, the standard deviation from 10 measurements is indicated in the parenthesis.

more sophisticated edge-detection subroutines may also be used to distinguish roughness from the nanostructures. We used such schemes and found that our algorithm was insensitive to the roughness using the 150 pixel value threshold mentioned earlier.

Table 1 shows the $d(\text{Image}||\text{HEX})$ metric comparing each image in Figure 1 to a standard hexagonal pattern. Table 1 then shows the *d-metric* could be a quantitative measure of the extent of dispersion, yielding progressively larger values for images that exhibit greater clustering/poor dispersion and deviating more from the chosen hexagonal lattice standard. The numerical values are indicative of the number of bits representing the difference/distance between the given and the standard distribution.[27]

We also compared the utility of the $d(P||Q)$ metric with other results from the literature (Figure 2—taken from [25] and Figure 3—taken from [22]). In the former paper, the importance of reducing particle size to increase the degree of matrix/polymer reinforcement was discussed.[30] We analyzed the micrographs indicating the nanoparticle dispersions in Figure 2, taken from the paper by Khare and Burris,[25] using our *d*-metric approach. While the general procedure was discussed earlier in the section, through (A)–(E), we outline the specific methodology. For example, in Figure 2(a), subsequent to the assignment of pixel values, i.e. 0 (black) and 255 (white), multiple quadrats each of size 50 nm square (corresponding to twice the length scale of the dots) was superimposed on and covered the image. The choice of 50 nm was dictated by reproducible dispersion metric results in addition to a reasonable computation time,
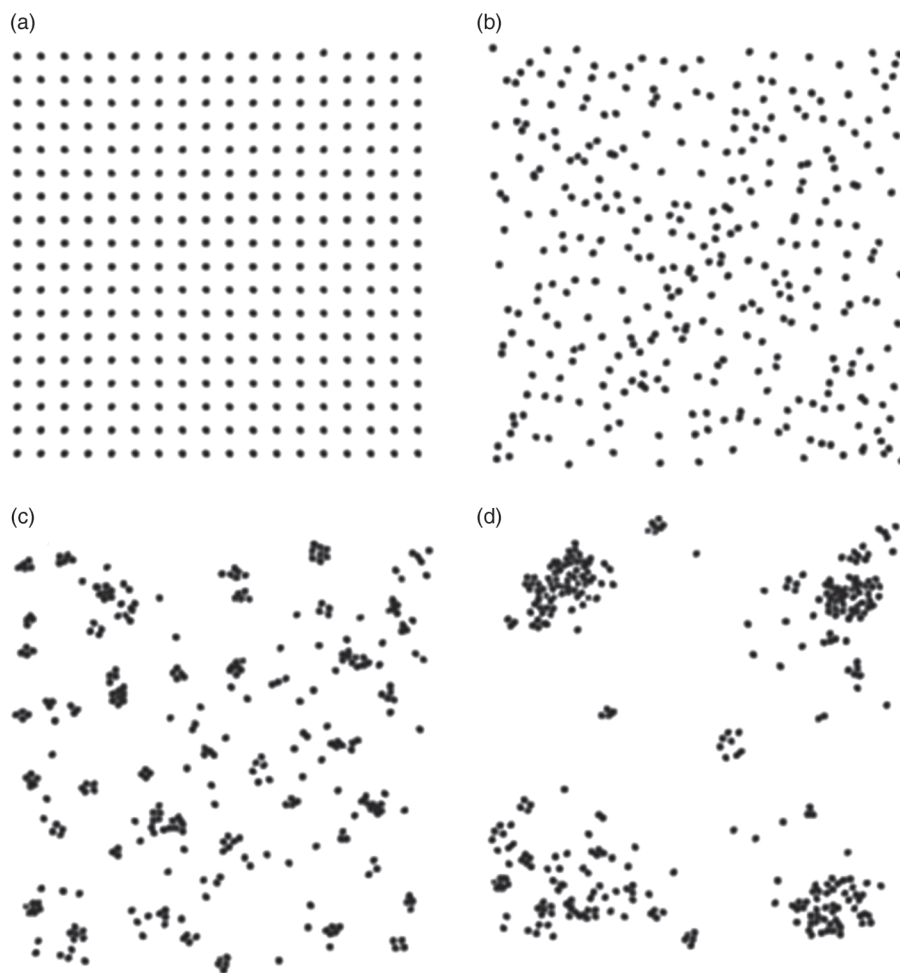
Figure 2.   Our proposed d-metric can be used to analyze the dispersion of nanoparticles, as well and indicates steadily decreasing uniformity from (a) to (d)—Table 2. (Image taken from the paper by Khare and Burris [25].)

per (D) and (E) in the general procedure. The feature distribution probabilities, (f_p)—see Equation (1), related to finding the specific feature/dots within the ith quadrat, were determined through using the area a_i (in units of pixels) of the feature within the ith quadrat of area $A_i(= 50\,\text{nm} \times 50\,\text{nm} = 2500\,\text{nm}^2)$ through Equation (4). The H (P) was obtained from Equation (1). Concomitantly, H (Q), with Q as a hexagonal distribution was computed (using a 50 nm quadrat size). The d-metric was estimated from Equations (2) and (3). Ten measurements of $d(P||Q)$, with respect to the HEX pattern, were averaged for any particular image/pattern under test to estimate the population average and lower the standard error estimate. In the other micrographs—Figure 2(b)–(d), an identical method to that discussed above was again used to obtain the respective d-metric values. The obtained results are indicated in Table 2. The comparison is now to a uniform distribution, with an implicit assumption that this is the desired distribution. The steadily increasing d-metric values from the top to the bottom, in the order (a) < (b) < (c) < (d), are in accordance with

the easily observed diminished uniformity of dispersion and indicate a quantifiable measure. It is interesting to note, from Table 2 that $\langle d(\text{Uniform}||a\rangle = 0.021$ and not zero. The d-metric value would exactly be zero only if all of the 10,000 randomly positioned quadrats (see the beginning of Section 3, in our paper) happen to encompass/circumscribe an equal number of particles (/dark pixels representing the particles). In more detail, in Figure 2(a), some randomly placed quadrats may superimpose over the gaps between the particles while other randomly positioned quadrats superimpose over the particle pixels. Consequently, the number of particle pixels circumscribed by each quadrat will not always be the same and accounts for $d(\text{Uniform}||a) \neq 0$.

In yet another study taken from the literature, the dispersion of alumina nanoparticles in a polyethylene terephthalate (PET) polymer matrix was investigated [22] through sample cross-sections taken from the composite (as given in Figure 3). The authors' analysis of the degree of dispersion was considered inadequate, as there was no obvious discrimination between
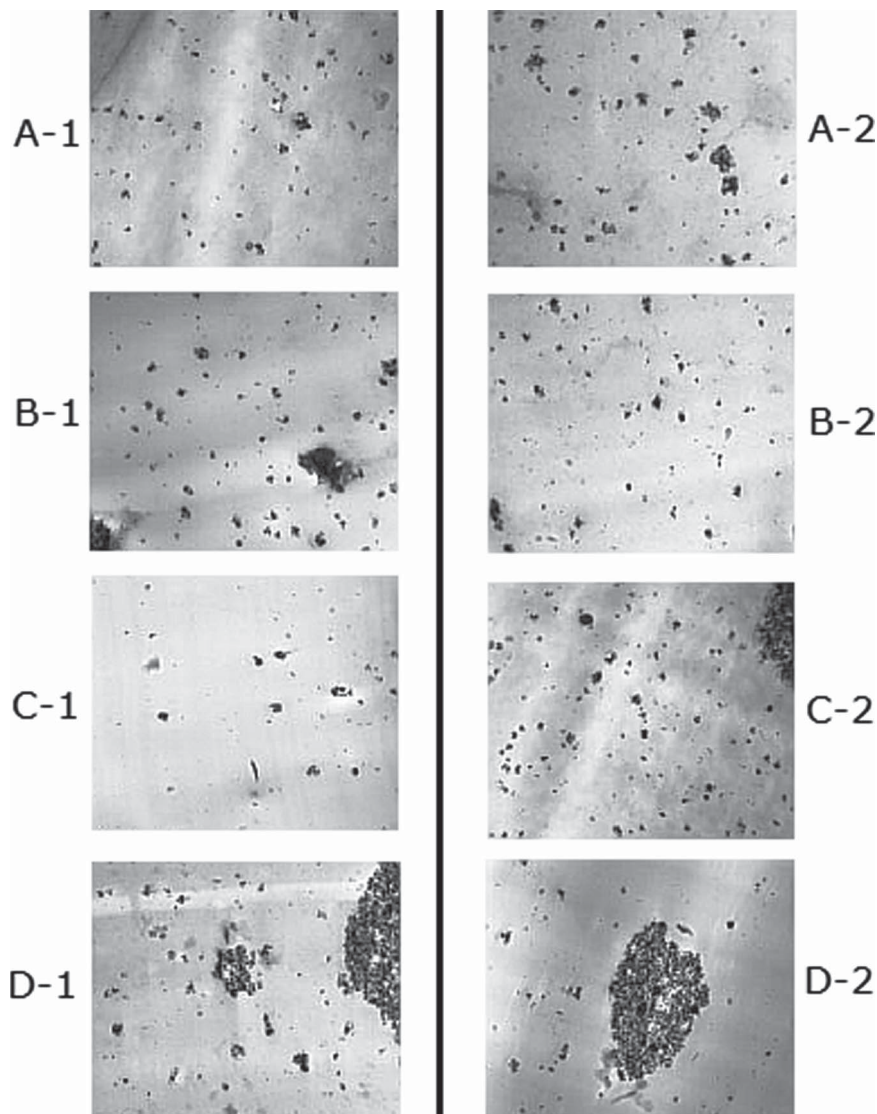
Figure 3.   Another example of the application of the *d*-metric to the dispersion of alumina nanoparticles in PET polymer through the analysis of a TEM image from the literature (Image taken from the paper by Kim et al. [22]). The non-uniformity of dispersion increases from A1 to D1 and A2 to D2. The dispersion metric results are presented in Table 3.

single nanoparticles vs. an agglomeration of contiguous nanoparticles and in addition, no comparison was made to a standard/preferred pattern. We then applied our *d*-metric-based approach to Figure 3, with the results indicated in Table 3. The comparison is again to a hexagonal pattern distribution. The steadily increasing *d*-metric values from the top to the bottom, for both columns, now indicate definitive and well-founded values for the

Table 3.   The *d*-metric for the images in Figure 3 indicates a quantification of the degree/uniformity of dispersion.

$\langle d(\text{HEX}||\text{Pattern})\rangle$	$\langle d(\text{HEX}||\text{Pattern})\rangle$
$\langle d(\text{HEX}||\text{A-1})\rangle = \mathbf{0.293}(0.002)$	$\langle d(\text{HEX}||\text{A-2})\rangle = \mathbf{0.306}(0.001)$
$\langle d(\text{HEX}||\text{B-1})\rangle = \mathbf{0.468}(0.002)$	$\langle d(\text{HEX}||\text{B-2})\rangle = \mathbf{0.322}(0.001)$
$\langle d(\text{HEX}||\text{C-1})\rangle = \mathbf{0.710}(0.005)$	$\langle d(\text{HEX}||\text{C-2})\rangle = \mathbf{0.630}(0.002)$
$\langle d(\text{HEX}||\text{D-1})\rangle = \mathbf{0.717}(0.002)$	$\langle d(\text{HEX}||\text{D-2})\rangle = \mathbf{1.282}(0.004)$

Note: The numbers in bold indicate the *d*-metric values, the standard deviation from 10 measurements is indicated in the parenthesis.

degree of dispersion. While it may initially be surprising to note that the similar values of the *d*-metric values for Figure C-1 and Figure D-1, one way of rationalizing the values is that the large gaps between particles in the former are as far (in terms of the average relative entropy or distance) from pattern HEX as the large agglomerated clusters in the latter figure.

Our methodology may also be adapted for three-dimensional images. Cross-sections of two-dimensional section scans at varying depths can be combined into a collage and our algorithm applied without modification. Alternatively, each cross-section can be evaluated individually and the *d*-metric dispersions evaluated at increasing cross-sectional depths. Such an evaluation can be easily accomplished, for example, by plotting the *d*-metric on statistical control charts.[39] The algorithm also can be adapted to three-dimensional imaging techniques through replacing quadrats with cuboids and area fractions with volume fractions.

4. Conclusions

We have shown conclusively that the *d*-metric, based on Equation (3), can be used to satisfactorily describe nanostructure dispersion in polymer composites. The metric was applied to micrographs of CNT-polymer composites, taken from our own studies as well as from previous literature, and yields a measure of the degree of uniformity relative to a preferred/standard distribution. The proposed measure incorporates a firm mathematical basis and has the advantage that the deviation of a given distribution from a standard distribution can be quantitatively gauged.

Supplementary Online Material. A more detailed information on experiments is available at http://dx.doi. org/10.1080/21663831.2014.886629.

References

[1] Moniruzzaman M, Winey KI. Polymer nanocomposites containing carbon nanotubes. Macromolecules. 2006;39:5194–5205.

[2] Ajayan PM, Schadler LS, Giannaris C, Rubio A. Single-walled carbon nanotube-polymer composites: strength and weakness. Adv Mater. 2000;12:750–753.

[3] Park S-H, Theilmann P, Asbeck P, Bandaru PR. Enhanced electromagnetic interference shielding through the use of functionalized carbon nanotube-reactive polymer composites. IEEE Trans Nanotechnol. 2010;9:464–469.

[4] Park S-H, Thielemann P, Asbeck P, Bandaru PR. Enhanced dielectric constants and shielding effectiveness of, uniformly dispersed, functionalized carbon nanotube composites. Appl Phys Lett. 2009;94:243111.

[5] Chung DDL. Electromagnetic interference shielding effectiveness of carbon materials. Carbon N Y. 2001;39: 279–285.

[6] Pradhan B, Setyowati K, Liu H, Waldeck DH, Chen J. Carbon nanotube-polymer nanocomposite infrared sensor. Nanoletters. 2008;8:1142–1146.

[7] Bekyarova E, Thostenson ET, Yu A, Itkis ME, Fakhrutdinov D, Chou T-W, Haddon RC. Functionalized single-walled carbon nanotubes for carbon fiber-epoxy composites. J Phys Chem C. 2007;111:17865–17871.

[8] Park SH, Bandaru PR. Improved mechanical properties of carbon nanotube/polymer composites through the use of carboxyl-epoxide functional group linkages. Polymer (Guildf). 2010;51:5071–5077.

[9] Breuer O, Sundararaj U. Big returns from small fibers: a review of polymer/carbon nanotube composites. Polym Compos. 2004;25:630–645.

[10] Todd MG, Shi FG. Complex permittivity of composite systems: a comprehensive interphase approach. IEEE Trans Dielectr Electr Insul. 2005;12:601–611.

[11] Smith RC, Liang C, Landry M, Nelson JK, Schadler LS. The mechanisms leading to the useful electrical properties of polymer nanodielectrics. IEEE Trans Dielectr Electr Insul. 2008;15:187–196.

[12] Fiedler B, Gojny FH, Wichmann MHG, Nolte MCM, Schulte K. Fundamental aspects of nano-reinforced composites. Compos Sci Technol. 2006;66:3115–3125.

[13] Lee LJ, Zeng C, Cao X, Han X, Shen J, Xu G. Polymer nanocomposite foams. Compos Sci Technol. 2005;65:2344–2363.

[14] Kim KH, Jo WH. A strategy for enhancement of mechanical and electrical properties of polycarbonate/multi-walled carbon nanotube composites. Carbon N Y. 2009;47:1126–1134.

[15] Yeh MK, Tai NH, Lin YJ. Mechanical properties of phenolic-based nanocomposites reinforced by multi-walled carbon nanotubes and carbon fibers. Compos Part A. 2008;39:677–684.

[16] Lo'pez Manchado MA, Valentini L, Biagiotti J, Kenny JM. Thermal and mechanical properties of single-walled carbon nanotubes–polypropylene composites prepared by melt processing. Carbon N Y. 2005;43: 1499–1505.

[17] Tai NH, Yeh MK, Peng TH. Experimental study and theoretical analysis on the mechanical properties of SWNTs/phenolic composites. Compos B. 2008;39:926–932.

[18] Ni C, Chattopadhyay J, Billups WE, Bandaru PR. Modification of the electrical characteristics of single wall carbon nanotubes through selective functionalization. Appl Phys Lett. 2008;93:243113.

[19] Tasis D, Tagmatarchis N, Bianco A, Prato M. Chemistry of Carbon Nanotubes. Chem Rev. 2006;106: 1105–1136.

[20] Pfeifer S, Park SH, Bandaru PR. Analysis of electrical percolation thresholds in carbon nanotube networks using the Weibull probability distribution. J Appl Phys. 2010;108:24305.

[21] Subcommittee: D24.71. ASTM D2663-08 (Standard test methods for carbon-black dispersion in Rubber) [Internet]. Am Soc Test Mater Digit Libr. 2014. Available from: enterprise.astm.org.

[22] Kim D, Lee JS, Barry CMF, Mead JL. Microscopic measurement of the degree of mixing for nanoparticles in polymer nanocomposites by TEM images. Microsc Res Technol. 2007;70:539–546.

[23] Rogers A. Statistical analysis of spatial dispersion: the quadrat method. London, UK: Pion Ltd.; 1974.

[24] Haslam MD, Raeymaekers B. A composite index to quantify dispersion of carbon nanotubes in polymer-based composite materials. Compos Part B. 2013;55:16–21.

[25] Khare HS, Burris DL. A quantitative method for measuring nanocomposite dispersion. Polymer (Guildf). 2010;51:719–729.

[26] Morisita M. Iq index, a measurement of dispersion of individuals. Res Popul Ecol (Kyoto). 1962;4:1–7.

[27] Cover TM, Thomas JA. Elements of information theory. Hoboken, NJ: Wiley-Interscience; 2006.

[28] Johnson D, Sinanovic S. Symmetrizing the Kullback-Leibler distance. Houston, TX: Rice University; 2001.

[29] Leon-Garcia A. Probability and random processes for electrical engineering. 2nd ed. Reading, MA: Addison-Wesley; 1994.

[30] Cencov NN. Statistical decision rules and optimal inference. Providence, RI: American Mathematical Society; 1982.

[31] Curtis JT, McIntosh RP. The interrelations of certain analytic and synthetic phytosociological characters. Ecology. 1950;31:434–455.

[32] Feng D, Jin G. Introduction to condensed matter physics. Singapore: World Scientific Publishing Co. Plc. Ltd; 2005.

[33] Gonzalez RC, Woods RE. Digital image processing. 2nd ed. Upper Saddle River, NJ: Prentice-Hall, Inc.; 2002.

[34] Dabak AG. A geometry for detection theory. Department of Electrical and Computer Engineering Houston, TX: Rice University; 1992.

[35] Love CT, Gapin A, Karbhari VM. Interfacial adhesion in multi-walled carbon nanotube/reactive ethylene ter-polymer composites. Baltimore, MD: Society for the Advancement of Material and Process Engineering; 2007.

[36] Bandaru PR, Daraio C, Yang K, Rao AM. A plausible mechanism for the evolution of helical forms in nanostructure growth. J Appl Phys. 2007;101:94307.

[37] Wang W, Yang K, Gaillard J, Bandaru PR, Rao AM. Rational synthesis of helically coiled carbon nanowires and nanotubes through the use of Tin and indium catalysts. Adv Mater. 2008;20:179–182.

[38] Sun L, Warren GL, O'reilly JY, Everett WN, Lee SM, Davis D, Lagoudas D, Sue HJ. Mechanical properties of surface-functionalized SWCNT/epoxy composites. Carbon N Y. 2008;46:320–328.

[39] Chambers DS, Wheeler DJ. Understanding statistical process control. 2nd ed. Knoxville, TN: SPC Press; 1992.